SPATA7: Evolving Phenotype from Cone-Rod Dystrophy to Retinitis Pigmentosa

Rodrigo Matsui[1], **David B. McGuigan III**[1], **Michaela L. Gruzensky**[1], **Tomas S. Aleman**[1], **Sharon B. Schwartz**[1], **Alexander Sumaroka**[1], **Robert K. Koenekoop**[2], **Artur V. Cideciyan**[1], and **Samuel G. Jacobson**[1,*]

[1]Scheie Eye Institute, Department of Ophthalmology, Perelman School of Medicine at the University of Pennsylvania, Philadelphia, Pennsylvania 19104, USA

[2]McGill Ocular Genetics Laboratory (MOGL), Departments of Paediatric Surgery, Human Genetics and Ophthalmology, Montreal Children's Hospital, McGill University Health Center, Montreal, Quebec, Canada

Abstract

Background—*SPATA7* mutation*s* have been associated with different autosomal recessive retinal degeneration phenotypes. Long-term follow-up has not been described in detail.

Materials and methods—A Hispanic patient with *SPATA7* mutations was evaluated serially over a 12-year period with kinetic and static chromatic perimetry, optical coherence tomography (OCT) and fundus autofluorescence (AF) imaging. Electroretinography (ERG) was performed at the initial visit.

Results—The patient was homozygous for a mutation in *SPATA7* (p.V458fs). At age 9, the ERG showed an abnormally reduced but preserved rod b-wave but no detectable cone signals. There were two islands of vision: a midperipheral island with greater cone than rod dysfunction and a central island with normal cone but no rod function. Serial measures of rod and cone vision and co-localized retinal structure showed that the midperipheral island slowly became undetectable. By age 21, only the central island and its cone function remained, but it had become more abnormal in structure and function.

Conclusion—The disease resulting from *SPATA7* mutations in this patient initially presented as a cone-rod dystrophy (CRD), but changed over time into a phenotype more reminiscent of late-stage retinitis pigmentosa (RP). The differential diagnosis for both CRD and RP should include this rare molecular cause of autosomal retinal degeneration. An evolving phenotype complicates not only clinical diagnosis and patient counselling but also future strategies aimed at treating specific retinal regions.

*To whom correspondence should be addressed at: Scheie Eye Institute, University of Pennsylvania, 51 N. 39th Street, Philadelphia, PA 19104, USA. Tel: +1 215 662 9981; Fax: +1 215 662 9388; jacobsos@mail.med.upenn.edu.

DECLARATION OF INTEREST

The authors report no conflict of interest and are responsible for the content and writing of the paper.

Keywords

cone rod dystrophy; optical coherence tomography; perimetry; rod; cilium; cone

INTRODUCTION

The underlying gene for the LCA3 locus on chromosome 14q24[1] is now known to be *SPATA7 (spermatogenesis-associated protein 7)*.[2] The expression of *SPATA7* has been localized to the photoreceptor connecting cilium. The main function of SPATA7 is involved in protein trafficking, including the correct localization of rhodopsin from the inner to the outer segments. The mislocalization of rhodopsin to the inner segments is likely to be the main defect that triggers cell degeneration in the retinopathy caused by *SPATA7* mutations.[2]

The original clinical description of patients now known to have *SPATA7* mutations was that of autosomal recessive Leber congenital amaurosis (LCA), but as more individuals were molecularly identified, other phenotypes were described.[3–6] Based on a functional classification, two main forms of *SPATA7*-retinopathy have been described in the literature: the first one was characterized as having rods more severely affected than cones (i.e. rod-cone dystrophy)[4] and a second form showed cones to be more severely affected than rods (i.e. cone-rod dystrophy).[5] With some exceptions,[5,6] most of the phenotype data are descriptions of patients at their single visits to a clinic.

We had the opportunity to examine clinically and with visual function and retinal imaging the natural history over a 12-year span of a patient with *SPATA7* mutations. We noted an unexpected change from a cone-rod dystrophy (CRD) phenotype to a presentation more like severe RP with unmeasurable function other than preserved visual acuity with central retinal lamination. Our case highlights how an evolving phenotype complicates accurate clinical diagnosis and the ability to provide counselling to a patient and their family; and it lends support to the argument for broad molecular DNA testing to complement ophthalmic testing.[7] Given increasing treatment options for rare diseases, a diagnosis made at an earlier rather than later disease stage could become vision-saving.

CASE REPORT

A 9-year-old asymptomatic Hispanic boy presented with a diagnosis of RP which was made two years earlier on a routine eye examination. At that time, retinal pigmentary changes were observed by funduscopy and there was an abnormal ERG. We performed complete examinations at ages 9,11,13,17 and 21. At age 9, best-corrected visual acuities were 20/25 (with a −1.50 refraction) OD and 20/32 (with a −1.25 +0.50 × 180° refraction) OS. Color vision with a Farnsworth D15 panel was normal. There was no nystagmus or anterior segment abnormalities. Funduscopy showed a waxy-appearing optic nerve head, minimal vessel attenuation, a bull's eye-like change in the macula and a tigroid appearance to the periphery. A standard full-field ERG showed reduced rod-mediated b-wave amplitudes, mixed cone-rod ERG with reduced a- and b-waves, and non-detectable cone-mediated responses (Figure 1A). Kinetic fields with the V-4e target were limited to a small (<5°) central island of vision and a midperipheral island of vision (Figure 1B). The ERG and

visual field data were consistent with a cone-rod dystrophy (CRD).[8,9] Serial data over 12 years showed progressive loss of the midperipheral island of vision by kinetic perimetry and further constriction of the residual central island (Figure 1B). By age 17, vision was detectable only near fixation. Visual acuity remained stable but refractive error became more myopic by about 1.50 diopters.

Molecular screening for mutations in 163 retinal disease genes was performed by next generation sequencing (See Supplementary Table 1). The only mutations found were in the known retinal disease gene *SPATA7*. These homozygous *SPATA7* mutations (c.1373del, p.V458fs) were then confirmed by Sanger sequencing.[10] Cosegregation studies were then performed and the parents were both heterozygous for this change. There was no parental consanguinity known. The p.V458fs mutation is one of sixteen known mutations associated with retinal degeneration reported to date in *SPATA7* (See Supplementary Figure S1).

Rod- and cone-mediated function was also explored with chromatic static perimetry (dark-adapted with 500- and 650-nm stimuli; light-adapted with 600-nm stimulus; 200-ms duration, 1.7° diameter target). Mediation by rod or cone photoreceptors was determined by comparison of dark-adapted sensitivities to the 500- and 650-nm stimuli.[11–13] Sensitivities were measured on a 12° grid across the field and at 2° intervals along vertical and horizontal meridians. Sensitivity profiles at age 9 revealed a central island of near normal, cone-mediated function separated from a nasal field island of near normal rod vision but abnormal cone function by an absolute scotoma (Figure 1C). The nasal field island diminished in rod and cone sensitivity within 4 years and was not detectable at age 17; the central cone island persisted. Remnants of midperipheral cone-mediated function observed at this location at age 9 were no longer detectable at age 13 (Figure 1C).

Maps of rod and cone sensitivity loss provide a view of the disease topography and its progression over the 12-year span (Figure 1D). At age 9, there was measurable rod more than cone function in the midperiphery beyond a dense pericentral scotoma surrounding the island of cone function at fixation; the extracentral function was consistent with the CRD-type ERG findings. At later visits, there was increasing rod and cone dysfunction and by age 17 (and 21, not shown) rod function was not detectable whereas cone function remained measurable at fixation. The pattern of retinal dysfunction at ages 17 and 21 was consistent with RP.[13]

What is the retinal structure underlying this pattern of dysfunction? OCT retinal cross-sections were acquired at all visits (age 9 and 11: time-domain OCT3, Carl Zeiss Meditec, Inc., Dublin, CA, USA; ages 13–21: spectral-domain OCT, RTVue-100; Optovue Inc., Fremont, CA, USA). Scans were along the horizontal and vertical meridians with the fovea at the center and were analyzed as published;[14–16] co-localized rod and cone sensitivities were also measured and shown above the scans (Figure 2). At age 9, foveal anatomy appeared normal and, as previously documented (Figure 1), there was mainly cone function retained in and near the fovea. Outer nuclear layer (ONL) thickness became reduced with increasing distance from the fovea and was not detectable between ~8° and 20°. At greater eccentricities, there was near normal lamination with both ONL and outer photoreceptor sublaminae becoming detectable. There was also normal rod but abnormal cone sensitivities.

At age 11, there was ONL thinning and associated vision loss at the inferior retinal region that had detectable structure and function at age 9 (Figure 2B); superior retina was less affected, and least affected was the temporal retinal region (Figure 2A). At age 21, ONL was detectable only near the foveal center in a small island with cone-mediated function. Magnified images of the relatively preserved regions in superior retina illustrate a sequence of structural changes, particularly those distal to the ONL (Figures 2B, 2C). The signal originating from the rod outer segments (ROS) is clearly visible at age 9. Only two years later, there is ONL and ROS thinning. At ages 13 to 21, ONL is barely detectable and OS unmeasurable (Figure 2C). Serial ONL thickness data are plotted as a function of eccentricity (Figure 2A–C, lowest panels).

En face imaging was performed with a confocal scanning laser ophthalmoscope (HRA2 or Spectralis HRA; Heidelberg Engineering, Heidelberg, Germany) between ages 11 to 21 using near infrared (NIR) excitation lights in reflectance (REF) and reduced-illuminance autofluorescence imaging (RAFI) modes.[17] At ages 11 and 13, there was a central elliptical region of relatively homogeneous high signal on NIR-RAFI (Figure 3A, main panels) and relatively low signal on NIR-REF (Figure 3A, insets). This pattern is thought to represent retained RPE melanization.[18] Immediately surrounding this central region was a heterogeneous pattern of hyper- and hypoautofluorescence associated with increased visibility of choroidal vessels. The combination of increased NIR-REF signal and reduced NIR-RAFI signal intensity, and choroidal visibility is likely to be associated with either depigmentation or loss of RPE.[18] At subsequent visits, there was a progressive constriction of the central elliptical region (Figure 3A). At age 21, a distinctly darker cresent had formed in the inferior parafovea as the region with brighter and homogeneous NIR-RAFI signal had become delimited only to the immediate foveal region. Wide-angle NIR-RAFI imaging was performed at two ages. Temporal to the macula, a region of relatively homogeneous high signal was apparent at age 11 (Figure 3B, arrows) but this feature was not visible by age 21.

DISCUSSION

Previous descriptions of the phenotype associated with *SPATA7* mutations include a severe, childhood-onset disease in the category of LCA, with early loss of central vision, hyperopia, nystagmus, bull's eye maculopathy, and progression to light perception,[1,3–5] as well as juvenile-onset or even later-onset RP-like phenotypes.[3,5,6,19] Syndromic forms of *SPATA7*-associated disease with extra-ocular manifestations have also been reported.[5] In some patients with measurable ERGs, a CRD clinical diagnosis was made based on non-detectable cone ERGs and severely abnormal rod function.[5] Serial functional and structural data in the patient reported here provides a rare glimpse of a transformation of a CRD phenotype into an RP phenotype. Our CRD diagnosis at presentation was based on the cone>rod dysfunction of the midperiphery (reflected in both perimetry and ERG); the surviving cone central island was an inconsistent feature at the time although it has been reported in some CRD patients.[9] After the degeneration of the midperiphery, the central cones were the vestige of function that made the phenotype appear to be end-stage RP. Such an evolution has not been previously documented; more commonly, clinical experience is with evolution through stages of increasing disease severity within one pattern of retinal degeneration.[13] Taken together with the reports of different phenotypes in *SPATA7* genotypes, the present

case of an evolving phenotype raises the larger question about how general or specific a gene screening search should be and whether a definitive clinical diagnosis should dictate a specific group of genetic tests. In other words, should a clinical diagnosis of CRD prompt a genetic testing exercise of currently known CRD genes, or should we test all known retinal genes? Currently, cost must also be factored into such decisions.[7]

Before the present era of emerging therapies for otherwise incurable genetic retinal degenerations, a discussion over speed and accuracy of clinical and molecular genetic diagnoses had little or no potential clinical or therapeutic impact. Sufficient understanding of the disease would be adequate to advise patient and family about prognosis, as well as inform them of the chances of further disease inheritance within the same generation or other generations. If there had been an opportunity to treat the condition at age 9 in our patient, however, there would have been far more retinal function and structure to treat.

A recent report of efficacy for subretinal gene therapy in the *Spata7* knockout mouse is encouraging although the issue of long-term continuing retinal degeneration needs further research.[20] A strategy for treating only the residual central island now at age 21 could represent a different challenge and intravitreal delivery of vector (or another therapy) may be more appropriate for remaining fragile central photoreceptors.[16]

Supplementary Material

Refer to Web version on PubMed Central for supplementary material.

Acknowledgments

References

1. Stockton DW, Lewis RA, Abboud EB, et al. A novel locus for Leber congenital amaurosis on chromosome 14q24. Hum Genet. 1998; 103:328–333. [PubMed: 9799089]

2. Eblimit A, Nguyen TM, Chen Y, et al. Spata7 is a retinal ciliopathy gene critical for correct RPGRIP1 localization and protein trafficking in the retina. Hum Mol Genet. 2015; 24:1584–1601. [PubMed: 25398945]

3. Wang H, den Hollander AI, Moayedi Y, et al. Mutations in SPATA7 cause Leber congenital amaurosis and juvenile retinitis pigmentosa. Am J Hum Genet. 2009; 84:380–387. [PubMed: 19268277]

4. Perrault I, Hanein S, Gerard X, et al. Spectrum of SPATA7 mutations in Leber congenital amaurosis and delineation of the associated phenotype. Hum Mutat. 2010; 31:E1241–1250. [PubMed: 20104588]

5. Mackay DS, Ocaka LA, Borman AD, et al. Screening of SPATA7 in patients with Leber congenital amaurosis and severe childhood-onset retinal dystrophy reveals disease-causing mutations. Invest Ophthalmol Vis Sci. 2011; 52:3032–3038. [PubMed: 21310915]

6. Avila-Fernández A, Cortón M, López-Molina MI, et al. Late onset retinitis pigmentosa. Ophthalmology. 2011; 118:2523–2524. [PubMed: 22136677]

7. Lee K, Garg S. Navigating the current landscape of clinical genetic testing for inherited retinal dystrophies. Genet Med. 2015; 17:245–252. [PubMed: 25790163]

8. Yagasaki K, Jacobson SG. Cone-rod dystrophy. Phenotypic diversity by retinal function testing. Arch Ophthalmol. 1989; 107:701–708. [PubMed: 2719580]

9. Szlyk JP, Fishman GA, Alexander KR, et al. Clinical subtypes of cone-rod dystrophy. Arch Ophthalmol. 1993; 111(6):781–788. [PubMed: 8512479]

10. Wang X, Wang H, Sun V, et al. Comprehensive molecular diagnosis of 179 Leber congenital amaurosis and juvenile retinitis pigmentosa patients by targeted next generation sequencing. J Med Genet. 2013; 50:674–688. [PubMed: 23847139]

11. Jacobson SG, Voigt WJ, Parel JM, et al. Automated light- and dark- adapted perimetry for evaluating retinitis pigmentosa. Ophthalmology. 1986; 93:1604–1611. [PubMed: 3808619]

12. Roman AJ, Schwartz SB, Aleman TS, et al. Quantifying rod photoreceptor-mediated vision in retinal degenerations: dark-adapted thresholds as outcome measures. Exp Eye Res. 2005; 80:259–272. [PubMed: 15670804]

13. Jacobson SG, Roman AJ, Aleman TS, et al. Normal central retinal function and structure preserved in retinitis pigmentosa. Invest Ophthalmol Vis Sci. 2010; 51:1079–1085. [PubMed: 19797198]

14. Huang Y, Cideciyan AV, Papastergiou GI, et al. Relation of optical coherence tomography to microanatomy in normal and rd chickens. Invest Ophthalmol Vis Sci. 1998; 39:2405–2416. [PubMed: 9804149]

15. Aleman TS, Cideciyan AV, Sumaroka A, et al. Retinal laminar architecture in human retinitis pigmentosa caused by Rhodopsin gene mutations. Invest Ophthalmol Vis Sci. 2008; 49:1580–1590. [PubMed: 18385078]

16. Jacobson SG, Cideciyan AV, Huang WC, et al. TULP1 mutations causing early-onset retinal degeneration: preserved but insensitive macular cones. Invest Ophthalmol Vis Sci. 2014; 55:5354–5364. [PubMed: 25074776]

17. Cideciyan AV, Swider M, Aleman TS, et al. Reduced-illuminance autofluorescence imaging in ABCA4-associated retinal degenerations. J Opt Soc Am A Opt Image Sci Vis. 2007; 24:1457–1467. [PubMed: 17429493]

18. Cideciyan AV, Swider M, Jacobson SG. Autofluorescence imaging with near-infrared excitation: normalization by reflectance to reduce signal from choroidal fluorophores. Invest Ophthalmol Vis Sci. 2015; 56:3393–3406. [PubMed: 26024124]

19. Kannabiran C, Palavalli L, Jalali S. Mutation of SPATA7 in a family with autosomal recessive early-onset retinitis pigmentosa. J Mol Genet Med. 2012; 6:301–303. [PubMed: 23300508]

20. Zhong H, Eblimit A, Moayedi Y, et al. AAV8(Y733F)-mediated gene therapy in Spata7 knockout mouse model of Leber congenital amaurosis and retinitis pigmentosa. Gene Ther. 2015; 22:619–627. [PubMed: 25965394]
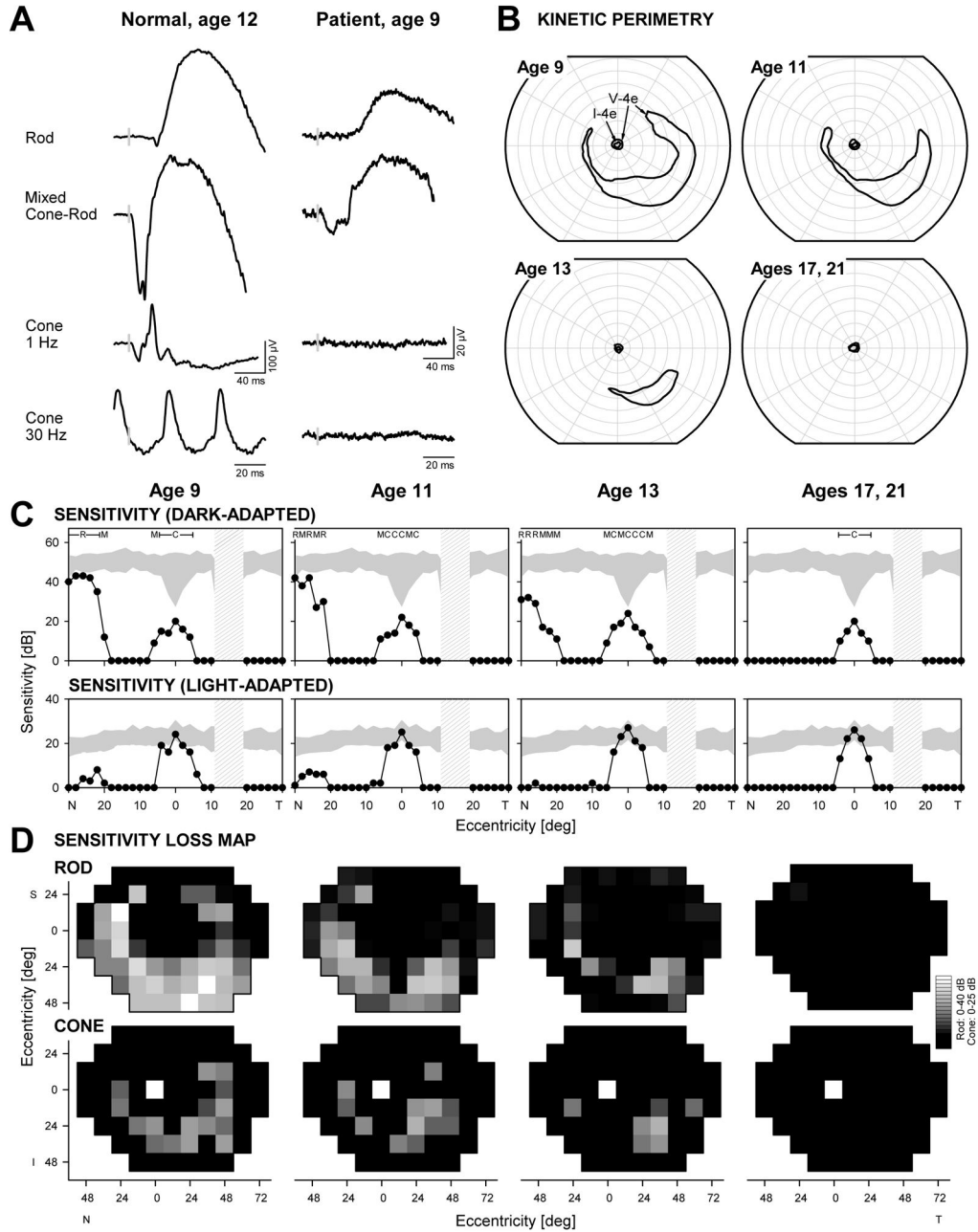
FIGURE 1.

Visual function in a patient with *SPATA7* mutations. (A) Representative ERG waveforms from a normal subject (*left*) compared with those from the patient with *SPATA7* mutations at the initial visit. Vertical gray bars on the traces mark stimulus onset; calibration bars are at right and below the waveforms. (B) Serial kinetic visual fields over a 12-year follow-up period (right eye data shown). (C) Dark-adapted (500 nm, *top*) and light-adapted (600 nm, *bottom*) horizontal sensitivity profiles (*filled symbols*) compared with normal data (*shaded band*, mean ± 2SD). For dark-adapted sensitivities, photoreceptor mediation based on two-color (500 nm, 650 nm) testing is shown above the results: R, rod-mediated; M, mixed rod-

and cone-mediated; C, cone-mediated. *Hatched bar*: physiologic blind spot. (D) Serial maps of rod (500 nm dark-adapted, *top)* and cone (600 nm light-adapted, *bottom)* sensitivity losses across the visual field in the patient. Gray scale is shown to the right. N, nasal; T, temporal; I, inferior; S, superior visual field.
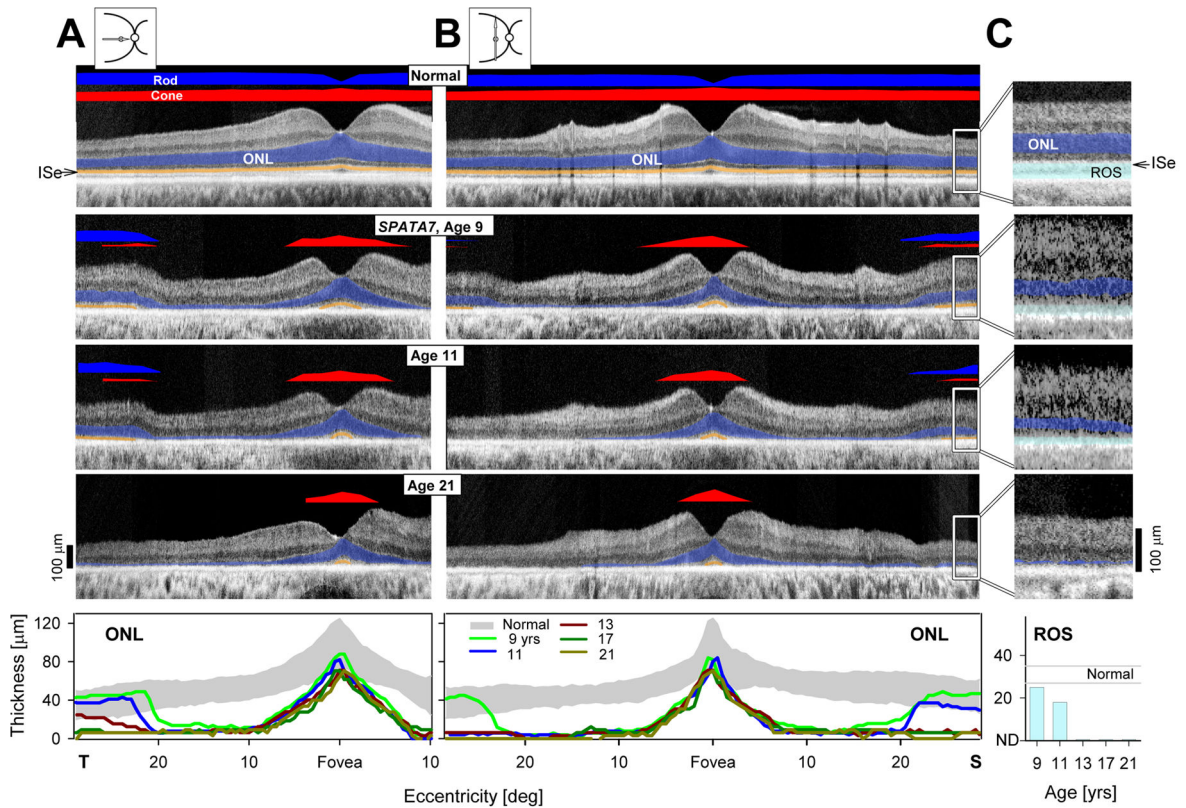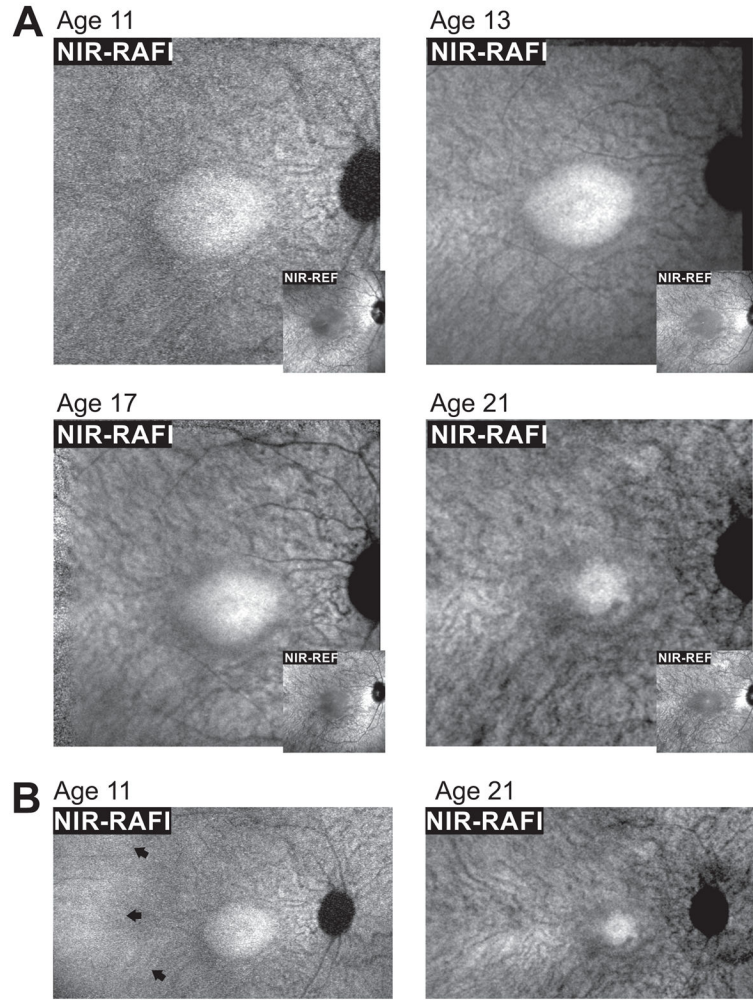
FIGURE 2.

Serial changes in retinal structure in the patient with *SPATA7* mutations. (A,B) Serial OCT cross-sections along the horizontal (A) and vertical (B) meridians through the fovea from representative visits are compared with data from a normal subject. Icons to the left of the normal cross-sections show scan location on fundus schematic. Bars above the cross-sections indicate rod (blue bar; dark-adapted, 500-nm stimuli) and cone (red bar; light-adapted, 600-nm stimuli) sensitivity measured by chromatic static perimetry. Outer nuclear layer (blue) and outer segments (orange) are highlighted on the scans. Serial ONL thickness as a function of eccentricity (*shaded band*, normal mean ± 2SD), is shown below. T, temporal; S, superior retina. (C) Magnified OCT images from extrafoveal regions (20–30° superior retina) delineated by white rectangles on the images illustrate serial changes in retina. Rod outer segments (cyan) are highlighted. Serial rod outer segment thickness quantitation is shown below (C).

FIGURE 3.
Serial changes apparent using *en face* imaging with a decade of followup. (A) Near-infrared (NIR) excited reduced-illuminance autofluorescence imaging (RAFI, main panels) and reflectance (REF, insets) imaging of the macula in the patient with *SPATA7* mutations at ages 11, 13, 17 and 21. A central homogeneous-appearing elliptical region of higher NIR-RAFI signal and lower NIR-REF signal is surrounded by a heterogeneous region displaying visibility of choroidal blood vessels. (B) Digital composites of NIR-RAFI showing a region of relatively greater homogeneity temporal to the macula (arrows) at age 11 that is not detectable by age 21. Each image is individually contrast stretched to allow visibility of features. Images shown in Panel A are 30°×30° and those in Panel B are 51°×29°.